

## Experiment Report Form

**The double page inside this form is to be filled in by all users or groups of users who have had access to beam time for measurements at the ESRF.**

Once completed, the report should be submitted electronically to the User Office using the **Electronic Report Submission Application**:

*<http://193.49.43.2:8080/smis/servlet/UserUtils?start>*

### ***Reports supporting requests for additional beam time***

Reports can now be submitted independently of new proposals – it is necessary simply to indicate the number of the report(s) supporting a new proposal on the proposal form.

The Review Committees reserve the right to reject new proposals from groups who have not reported on the use of beam time allocated previously.

### ***Reports on experiments relating to long term projects***

Proposers awarded beam time for a long term project are required to submit an interim report at the end of each year, irrespective of the number of shifts of beam time they have used.

### ***Published papers***

All users must give proper credit to ESRF staff members and proper mention to ESRF facilities which were essential for the results described in any ensuing publication. Further, they are obliged to send to the Joint ESRF/ ILL library the complete reference and the abstract of all papers appearing in print, and resulting from the use of the ESRF.

Should you wish to make more general comments on the experiment, please note them on the User Evaluation Form, and send both the Report and the Evaluation Form to the User Office.

### **Deadlines for submission of Experimental Reports**

- 1st March for experiments carried out up until June of the previous year;
- 1st September for experiments carried out up until January of the same year.

### **Instructions for preparing your Report**

- fill in a separate form for each project or series of measurements.
- type your report, in English.
- include the reference number of the proposal to which the report refers.
- make sure that the text, tables and figures fit into the space available.
- if your work is published or is in press, you may prefer to paste in the abstract, and add full reference details. If the abstract is in a language other than English, please include an English translation.



**Experiment title: Mapping of silver nanoparticles in Ostrea Edulis**

**Experiment number:**  
EC 721

<b>Beamline:</b> ID21	<b>Date of experiment:</b> from: 8 <sup>th</sup> September 2010 to: 14 <sup>th</sup> September 2010	<b>Date of report:</b>
<b>Shifts:</b> 18	<b>Local contact(s):</b> Marine Cotte ( <a href="mailto:cotte@esrf.fr">cotte@esrf.fr</a> ) Murielle Salome ( <a href="mailto:salome@esrf.fr">salome@esrf.fr</a> )	<i>Received at ESRF:</i>

**Names and affiliations of applicants** (\* indicates experimentalists):

Dr. Lidija Siller  
Dr. D. Medakovic

## Report:

Engineered, manufactured, or synthesized nanomaterials (NMs) have unique properties that will likely lead to their widespread commercial use in near future. For example, silver nanoparticles have already found many applications.

NMs will enter the environment through the air, water and sediment during the commercial life cycle, from synthesis to disposal. Embryonic development of the sea urchin are of vast interest for ecotoxicology, cell biology, embryology and for biomineralization. In this work *Paracentrotus lividus* sea urchin have been exposed to silver nanoparticles, in order to investigate the influence of the nanomaterials on skeletogenesis in late stage and the fate of Ag nanoparticles in sea water. As control embryos reached the pluteus stage, treat embryos with silver showed an inhibition of skeletal elongation and patterning. The submicro imaging technique, the X-ray fluorescence microscopy, Fourier transform infra red (FTIR) microscopy and submicro X-ray absorption near-edge structure spectroscopy (XANES) at beam line ID 21 were used to make detailed chemical maps of malformation in sea urchins.

### *Experimental methods*

The image contrast in the scanning transmission X-ray microscope (STXM) is due to absorption of the incident X-rays. Experiments were carried out in which sample regions were first imaged with X-ray fluorescence mapping (XRF) was tuned to 3.56 keV the Ag L<sub>3</sub>- edge using a fixed-exit double crystal Si(111) monochromator. Typical size of the beam spot on the sample was 0.2 $\mu$ m x 0.8 $\mu$ m. Locally, in situ X-ray Absorption Near Edge Structure (XANES) spectra were collected in focused mode on selected points of the sample to assess Ag speciation at high spatial resolution (the spatial resolution is given by the size of the pixel which is 250nm x 250nm). XANES spectra were acquired in fluorescence mode (3.32 keV to 3.47 keV, 600 points) with 0.225 eV energy steps and 0.1s dwell time.

Although the primary beam energy was set to around that of the Ag L<sub>3</sub>- edge energy region, elements with absorption edges at lower energies were also subject to excitation and emission of fluorescence photons, and could therefore be determined. Thus, element maps of Mg, Cl, Si, P, S and Na were obtained simultaneously with the Ag map.

The synchrotron micro Fourier transform IR (FTIR) microscopy was performed on the IR end-station of the ID21 beam line at ESRF in transmission mode. The beamline is equipped with a Continuum IR microscope (Thermo Nicolet) coupled to a Nexus Fourier transform IR bench (Thermo Nicolet). The microscope operates in confocal mode, where the focusing Schwarzschild objective and the collection Schwarzschild objective have a magnification of x32 (numerical aperture 0.65). Owing to its reduced source size and high collimation properties, a synchrotron IR source is more efficiently coupled to the low acceptance of confocal microscope, while its higher spectral luminescence (brightness) allows signal-to-noise ratios to be kept at diffraction-limited resolutions. The microscope is equipped with a computer-controlled x/y stage allowing acquisition of profiles or maps of the sample. The spot size of the beam was 6µm x 6µm. Samples were deposited on 0.2mm thin BaF<sub>2</sub> window.

Synthesized silver nanoparticles solution was prepared by chemical reduction following the method used by Link et al. with minor changes [1]. Dynamics light scattering (DLS) was used for size and size distribution of silver NPs by Malvern HPPS 3.3 instrument. In addition, size was also checked by Transmission Electron Microscope (TEM, JEOL 2100F FGETEM, Durham University). The Cu grid with lacey carbon film (300 mesh, Agar Scientific) was added by 3 drops of each sample and was dry in the air at room temperature in TEM sample preparation. The HRTEM images show that average size of Ag nanoparticles (AgNPs) is average size ~40-60nm. The sea urchins were exposed to concentrations of AgNPs of 0.3 µg/ml in sea water.

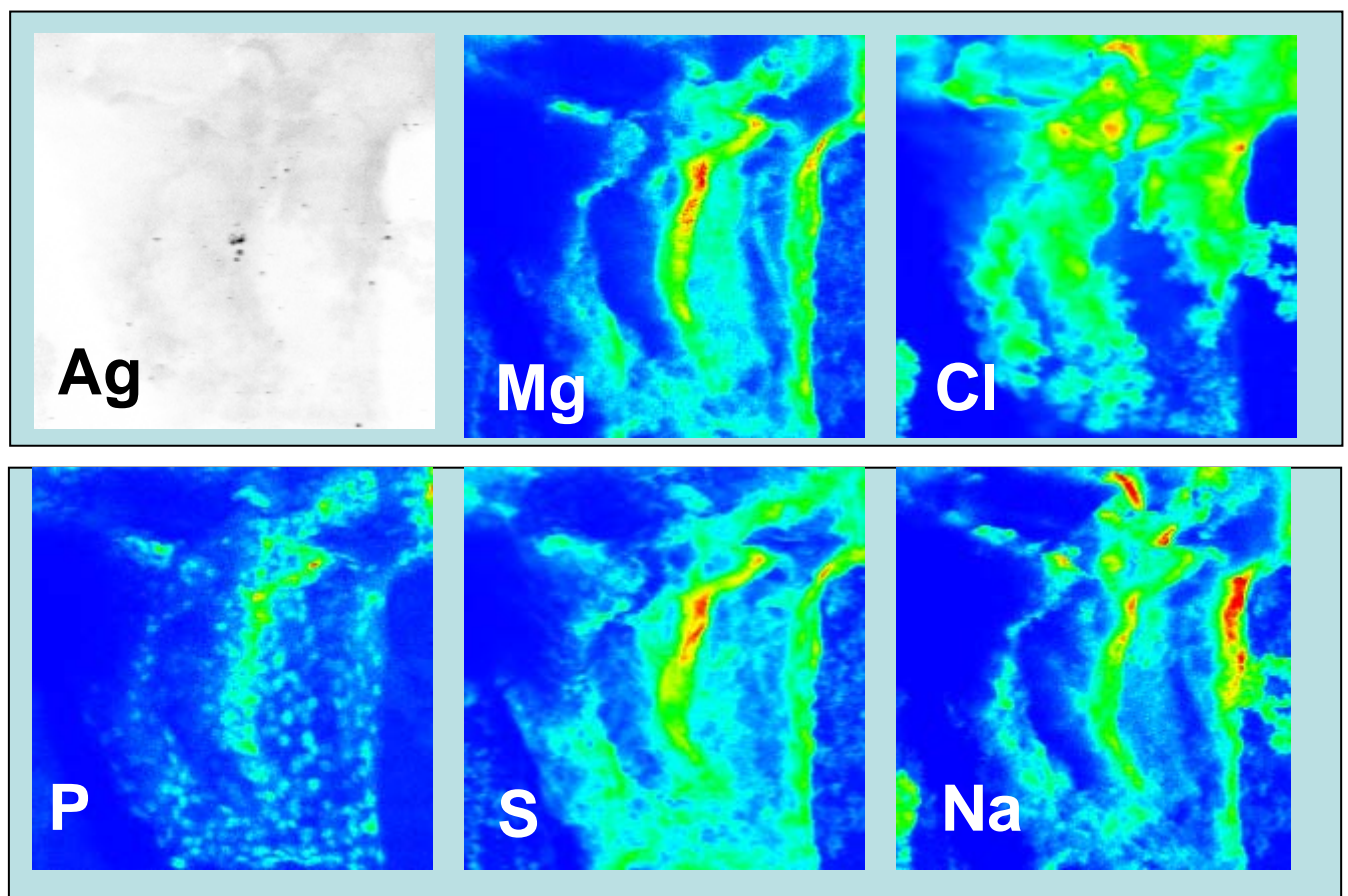


Figure 1 show X-ray fluorescence maps for Ag, Mg, Cl, P, S and Na of *Paracentrotus lividus* sea urchin exposed to average size ~40-60 nm Ag nanoparticles, with concentrations of 0.3 µg/ml in sea water.

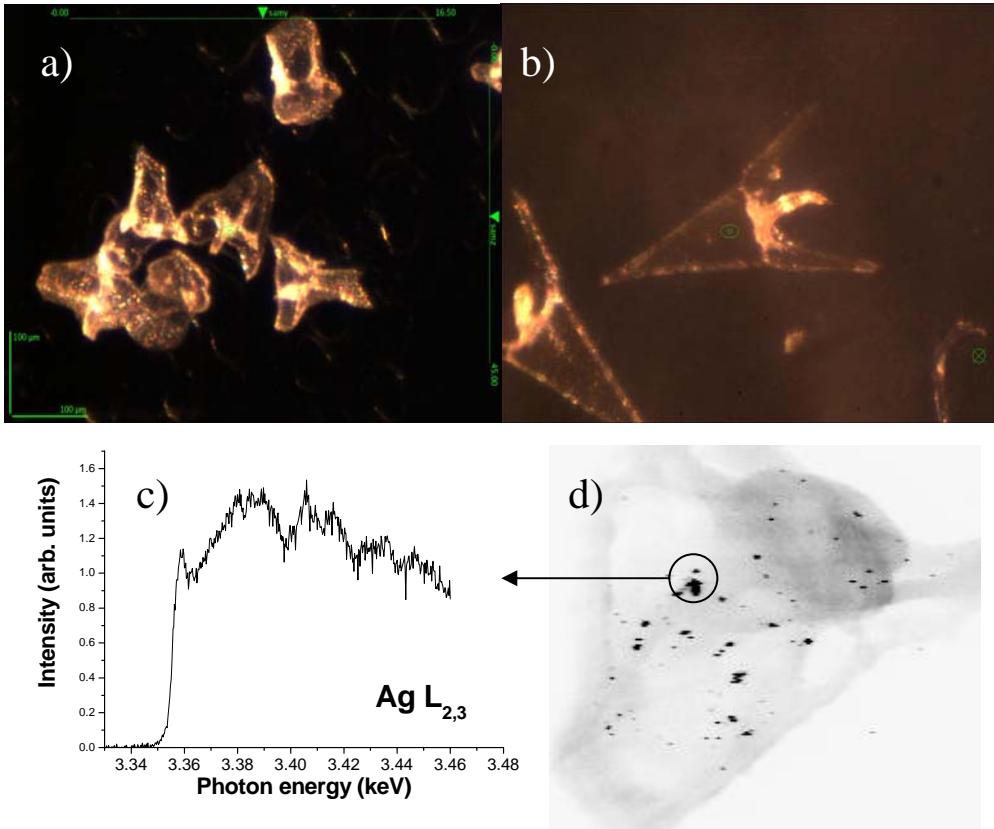


Figure 2 a) group of 8 *Paracentrotus lividus* sea urchins exposed to ~40-60 nm large Ag nanoparticles, with concentrations of 0.3  $\mu\text{g/ml}$  in sea water after 51 hour of growth (scale bar is  $100\mu\text{m} \times 100\mu\text{m}$ ) b) show Control sea urchin c) XANES spectra at Ag  $L_{2,3}$  edge at darkest area within the circle drawn in d). The beam spot size during XANES was collapsed to  $0.2\ \mu\text{m} \times 0.8\ \mu\text{m}$  (the size of the whole image is  $100\mu\text{m} \times 100\mu\text{m}$ ). d) the X-ray fluorescence map for Ag of sea urchin exposed to AgNPs as under a).

When we compare figure 2a with 2b, sea urchins exposed to AgNPs and control, respectively, we note that treated embryos showed a vast deficiency in skeletogenesis and arm elongation, in similar way as it has been observed when early blastule were exposed to antibody of an extracellular matrix (ECM) protein, i.e. anti-fibronectin [2]. Figure 1 shows X-ray fluorescence maps for Ag, Mg, Cl, P, S and Na of sea urchin exposed to ~40-60nm Ag nanoparticles, with concentrations of 0.3  $\mu\text{g/ml}$  in sea water. Clearly the agglomeration of Ag nanoparticles in upper part of the sea urchin has been detected. The XRF maps of different elements show different distributions which demonstrates that present thickness of the sample does not hinder chemical mapping of the sea urchin. In particular it is interesting to observe 'spoty' type distribution of P over sea urchin embryo. The same 'spoty' type distribution has been observed for control sample (not shown here) and therefore this is not due to presence of AgNPs itself but rather related to pluteous developmental stage of the sea urchin. It is known from biomineralisation that the P plays an important role in early stages of the growth of skeletogen so we suggest that the observed 'spoty' distribution of P is a precursor for growth of the spicules on the surface of the sea urchin.

The silver agglomeration in XRF maps has been detected in every specimen which has been mapped (6 in total), but in control samples there was no Ag agglomeration (not shown here). In Figure 2d) we see large accumulation of Ag, and it is mainly concentrated in the upper part of the sea urchin as in Figure 1. Similar observation on other specimens have been done and therefore it is very likely that this Ag agglomerates are placed within the sea urchin and related to its stomach which is in the upper part. This would imply that AgNPs uptake in sea urchin occurs through the ingestion rather than through the skin. However further experiments such as tomography are needed in order to confirm this assumption.

In figure 2c) the distinctive edge peak appearing at the Ag  $L_3$  X-ray absorption edge is observed at 3.359 keV and according to recent work can be formally assigned to 2p to 5s transition [3]. It has been suggested that although the 2p-to-5s transition in itself is weak, the intensity is borrowed from 4d through the

5s-4d hybridization and that the edge peak intensity is directly related to the covalence between Ag and the ligands, which enhances the 5s-4d hybridization [3]. Since the shape of the edge is similar to Ag<sub>2</sub>O [3], this indicates that agglomerates of Ag in silver urchin are in hybridized form of Ag and O.

To investigate the detailed chemical changes in sea urchin we measure  $\mu$ FTIR of sea urchins exposed to AgNPs and control samples.

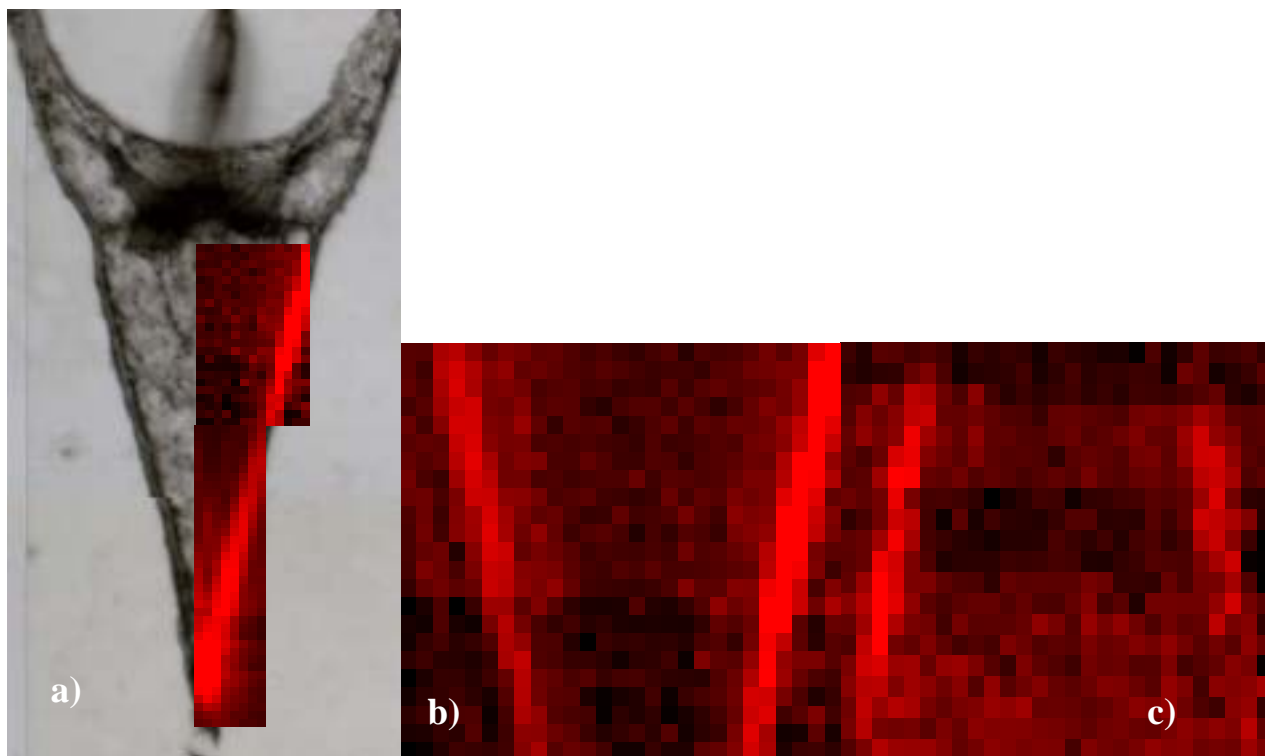


Figure 3.  $\mu$ FTIR map in transmission mode of a) 864 cm<sup>-1</sup> in control sea urchin and in b) 864 cm<sup>-1</sup> enlarged section of Control sea urchin c) 866 cm<sup>-1</sup> in sea urchin exposed to ~40-60 nm large AgNPs after 51 hour (image size is 108 $\mu$ m x 80 $\mu$ m). Samples were deposited on 0.2mm thin BaF<sub>2</sub> window. The mapping was carried with 4 $\mu$ m step size.

Vibrations at 1794 cm<sup>-1</sup>, 1465cm<sup>-1</sup> and 864 cm<sup>-1</sup> have been clearly observed in area over arms of sea urchin control sample and assigned to the calcite [4]. 864 cm<sup>-1</sup> which is carbonat out-of-plane bending ( $\nu_2$  mode) in calcite [5], has been plotted in Figure 3 for both control sample (Figure 3b) and sea urchin exposed to AgNPs (Figure 3c). We see that calcite is most strongly located over arms in sea urchin, but that the thickness of the arms in sea urchin exposed to AgNPs is much less pronounced indicating that the biomineralisation in sea urchin is strongly affected by presence of AgNPs during embryonal development. The integrated spectra over area of arms of sea urchin (not shown here) diminishes in intensity of all calcite related vibrations (1794cm<sup>-1</sup>, 1465cm<sup>-1</sup> and 864 cm<sup>-1</sup>). The band observed in control sample at 1070cm<sup>-1</sup> is missing in the sea urchin exposed to AgNPs but a new band at 1093cm<sup>-1</sup> appears. The band at 1093cm<sup>-1</sup> is likely to be due to larger presence of Amorphous Calcium Carbonate (ACC) phase [5]. In addition a new strong vibrational band at 1030 cm<sup>-1</sup> has been observed in sea urchin exposed to AgNPs.

## References

- [1] S. Link, Z.L. Wang and M.A. El-Sayed. *J. Phys. Chem. B*, 103, 3529-3533 (1999).
- [2] F. Zito, V. Tesoro, D.R. McCay, E. Nakano, V. Matranga, *Developmental Biology* 196, 184-192 (1998).
- [3] T. Miyamoto, H. Niimi, Y. Kitajima, T. Naito, and K. Asakura, *J. Phys. Chem.*, 114, 4093-4098 (2010).
- [4] G-T. Zhou, Y-B. Guan, Q-Z Yao and S-Q Fu, *Chem. Geol.*, 279, 63-72 (2010).
- [5] G-T. Zhou, J.C. Yu, X-C Wang and L-Z Zhang, *New J. Chem.*, 28, 1027 (2004).